

Square-Contact Representations of Partial 2-Trees and Triconnected Simply-Nested Graphs*

Giordano Da Lozzo, William E. Devanny, David Eppstein, and Timothy Johnson

Computer Science Department, University of California, Irvine, USA
 {gdalozzo,wdevanny,eppstein,tjohnso}@uci.edu

Abstract

A *square-contact representation* of a planar graph $G = (V, E)$ maps vertices in V to interior-disjoint axis-aligned squares in the plane and edges in E to adjacencies between the sides of the corresponding squares. In this paper, we study *proper* square-contact representations of planar graphs, in which any two squares are either disjoint or share infinitely many points.

We characterize the partial 2-trees and the triconnected cycle-trees allowing for such representations. For partial 2-trees our characterization uses a simple forbidden subgraph whose structure forces a separating triangle in any embedding. For the triconnected cycle-trees, a subclass of the triconnected simply-nested graphs, we use a new structural decomposition for the graphs in this family, which may be of independent interest. Finally, we study square-contact representations of general triconnected simply-nested graphs with respect to their outerplanarity index.

1998 ACM Subject Classification G.2.2 Graph Theory

Keywords and phrases Square-Contact Representations, Partial 2-Trees, Simply-Nested Graphs

1 Introduction

Contact representations of graphs, in which the vertices of a graph are represented by non-overlapping or non-crossing geometric objects of a specific type, and edges are represented by tangencies or other contacts between these objects, form an important line of research in graph drawing and geometric graph theory. For instance, the Koebe–Andreev–Thurston circle packing theorem states that every planar graph is a contact graph of circles [12]. Other types of contact representations that have been studied include contacts of unit circles [2, 8], line segments [9], circular arcs [1], triangles [7], L-shaped polylines [3], and cubes [6].

Schramm’s monster packing theorem [10] implies that every planar graph can be represented by the tangencies of translated and scaled copies of any smooth convex body in the plane. However, it is more difficult to use this theorem for non-smooth shapes, such as polygons: when k bodies can meet at a point, the monster theorem may pack them in a degenerate way in which separating k -cycles, and their interiors, shrink to a single point.

In this paper we study one of the simplest cases of contact representations that cannot be adequately handled using the monster theorem: contact systems of axis-parallel squares. We distinguish between *proper* and *improper* contacts: a *proper* contact representation disallows squares that meet only at their corners, while an *improper* or *weak* contact representation allows corner-corner contacts of squares. These weak contacts may represent edges of the graph,

* Supported in part by the National Science Foundation under Grants CCF-1228639, CCF-1618301, and CCF-1616248. This article also reports on work supported by the U.S. Defense Advanced Research Projects Agency (DARPA) under agreement no. AFRL FA8750-15-2-0092. The views expressed are those of the authors and do not reflect the official policy or position of the Department of Defense or the U.S. Government.



but they are also allowed between squares that should be non-adjacent. The weak contact representations by squares were shown by Schramm [11] to include all of the proper induced subgraphs of maximal planar graphs that have no separating 3-cycles or 4-cycles. However, a characterization of the graphs having proper contact representations by squares remains elusive.

There is a simple necessary condition for the existence of a proper contact representation by squares. No three properly-touching squares can surround a nonzero-area region of the plane. Therefore, if every embedding of a planar graph G with four or more vertices has a separating triangle or a triangle as the outer face, then G cannot have a proper contact representation. Our main results show that this necessary condition is also sufficient for two notable families of planar graphs: partial 2-trees (including series-parallel graphs) and triconnected cycle-trees (including the Halin graphs). However, we show that this necessary condition is not sufficient for the existence of weak and proper square-contact representations of 3-outerplanar and 2-outerplanar triconnected simply-nested graphs.

Due to space limits, full versions of omitted or sketched proofs are provided in [Appendix B](#).

2 Preliminaries

For standard graph theory concepts and definitions related to planar graphs, their embeddings, and connectivity we refer the reader, e.g., to [5] and to [Appendix A](#).

The graphs considered in this paper are planar, finite, simple, and connected. We denote the vertex set V and the edge set E of a graph $G = (V, E)$ by $V(G)$ and $E(G)$, respectively. Let H and G be two graphs. We say that G is H -free if G does not contain a subgraph isomorphic to H . The complete k -partite graph $K_{|V_1|, \dots, |V_k|}$ is the graph $(V = \bigcup_{i=1}^k V_i, E = \bigcup_{i < j} V_i \times V_j)$.

Series-parallel graphs and partial 2-trees. A *two-terminal series-parallel* graph G with source s and target t can be recursively defined as follows: (i) Edge st is a two-terminal series-parallel graph. Let G_1, \dots, G_k be two-terminal series-parallel graphs and let s_i and t_i be the source and the target of G_i , respectively, with $1 \leq i \leq k$. (ii) The *series composition* of G_1, \dots, G_k obtained by identifying s_i with t_{i+1} , for $i = 1, \dots, k-1$, is a two-terminal series-parallel graph with source s_k and target t_1 ; and (iii) the *parallel composition* of G_1, \dots, G_k obtained by identifying s_i with s_1 and t_i with t_1 , for $i = 2, \dots, k$, is a two-terminal series-parallel graph with source s_1 and target t_1 .

A *series-parallel graph* is either a single edge or a two-terminal series-parallel graph with the addition of an edge, called *reference edge* joining s and t . Clearly, series-parallel graphs are 2-connected. A series-parallel graph G with reference edge e is naturally associated with a rooted tree T , called the *SPQ-tree* of G . Each internal node of T , with the exception of the one associated with e , corresponds to a two-terminal series-parallel graph. Nodes of T are of three types: *S*-, *P*-, and *Q*-nodes. Further, tree T is rooted to the *Q*-node corresponding to e .

Let μ be a node of T with terminals s and t and children μ_1, \dots, μ_k , if any. Node μ has an associated multigraph, called the *skeleton* of μ and denoted by $skel_\mu$, containing a *virtual edge* $e_i = s_i t_i$, for each child μ_i of μ . Skeleton $skel_\mu$ shows how the children of μ , represented by “virtual edges”, are arranged into μ . The skeleton $skel_\mu$ of μ is: (i) edge st , if μ is a leaf *Q*-node, (ii) the multi-edge obtained by identifying the source s_i and the target t_i of each virtual edge e_i , for $i = 1, \dots, k$, with a new source s and a new target t , respectively, or (iii) the path e_1, \dots, e_k , where virtual edge e_i and e_{i+1} share vertex $s_i = t_{i+1}$, with $1 \leq i < k$. If μ is an *S*-node, then we denote by $\ell(\mu)$ the length of $skel_\mu$, i.e., $\ell(\mu) = k$.

Also, for each virtual edge e_i of $skel_\mu$, recursively replace e_i with the skeleton $skel_{\mu_i}$ of its corresponding child μ_i . The two-terminal series-parallel subgraph of G that is obtained in this way is the *pertinent graph* of μ and is denoted by G_μ . We have that G_μ is: (i) edge st , if μ is

a Q-node, (ii) the series composition of the two-terminal series-parallel graphs $G_{\mu_1}, \dots, G_{\mu_k}$, if μ is an S-node, and (iii) the parallel composition of the two-terminal series-parallel graphs $G_{\mu_1}, \dots, G_{\mu_k}$, if μ is a P-node. We denote by G_μ^- the subgraph of G_μ obtained by removing from it terminals s and t together with their incident edges.

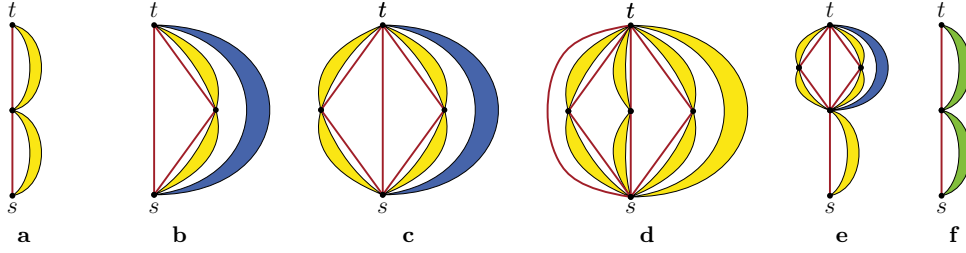
A *2-tree* is a graph that can be obtained from an edge by repeatedly adding a new vertex connected to two adjacent vertices. Every 2-tree is planar and 2-connected. A *partial 2-tree* is a subgraph of a 2-tree. Equivalently, *partial 2-tree* can be defined as the K_4 -minor-free graphs. In particular, the series-parallel graphs are exactly the 2-connected partial 2-trees.

Simply-nested graphs. Let G be an embedded planar graph and let G_1, \dots, G_k be the sequence of embedded planar graphs such that $G_1 = G$, G_{i+1} is obtained from G_i by removing all the vertices incident to the outer face of G_i together with their incident edges, and G_k is outerplanar. We say that the embedding of G is *k-outerplanar*. A graph is *k-outerplanar* if it admits a *k-outerplanar* embedding. The set V_i of vertices incident to the outer face of G_i is the *i-th level* of G . A *k-outerplanar* graph is *simply-nested* [4] if, for $i = 1, \dots, k-1$, graphs $G[V_i]$ are chordless cycles and $G[V_k]$ is either a cycle or a tree.

We define *cycle-trees* and *cycle-cycles* the 2-outerplanar simply-nested graphs whose internal level is a tree and a cycle, respectively. The 2-outerplanar 3-connected simply-nested graphs have a nice geometric interpretation. Similarly to the Halin graphs, which are the graphs of polyhedra containing a face that share an edge with all other faces, 3-connected cycle-trees are the graphs of polyhedra containing a face touched by all other faces. Analogously, the 3-connected cycle-cycle graphs with no chords on the inner cycle are the graphs of polyhedra in which there exist two disjoint faces that are both touched by all other faces.

Square-contact representations. Let $G = (V, E)$ be a planar graph. A *square-contact representation* Γ of G maps each vertex $v \in V$ to an axis-aligned square $S_\Gamma(v)$ in the plane, such that, for any two vertices $u, v \in V$, squares $S_\Gamma(u)$ and $S_\Gamma(v)$ are interior-disjoint, and the sides of $S_\Gamma(u)$ and $S_\Gamma(v)$ touch if and only if $uv \in E$. A square-contact representation of G is *proper* if any two touching squares share infinitely many points, i.e., they cannot share only a corner point, and *non-proper*, otherwise. When the square-contact representation is clear from the context, we may choose to drop the Γ subscript and just use $S(v)$ to refer to the square for vertex v . In the remainder of the paper, we only consider proper square-contact representations and refer to such representations simply as square-contact representations.

Geometric transformations. Let G be planar graph and let Γ be a square-contact representation of G . Also, let p be any point in Γ . We define the \nearrow -, \nwarrow -, \swarrow -, and \searrow -quadrant of p in Γ as the first, second, third, and fourth quadrant around p , respectively. Suppose that the half-lines delimiting the \swarrow -quadrant of p in Γ do not intersect the interior of any square in Γ . Also, let Γ' be the part of Γ lying in the \swarrow -quadrant of p . Then, a \swarrow -scaling of Γ by a factor $\alpha > 0$ is a square-contact representation Γ^* defined as follows; see, e.g., Fig. 3. Initialize $\Gamma^* = \Gamma$ and remove from Γ^* the drawing of the squares contained in the interior of Γ' . Then, insert into Γ^* a copy Γ'' of Γ' scaled by α such that the upper-right corner of Γ'' coincides with p . Clearly, depending on the scale factor α , drawing Γ^* may or may not be a square-contact representation of G (as adjacencies may be lost or gained). In the following, we refer to the case in which $\alpha > 1$ simply as a \swarrow -scaling of Γ and to the case in which $0 < \alpha < 1$ as a *negative \swarrow -scaling* of Γ . The definition of \nwarrow -scaling and *negative \nwarrow -scaling*, with $\circ \in \{\nwarrow, \swarrow, \nearrow\}$, is analogous. Finally, let v be a vertex of G and let x , y , z , and w be the upper-left, lower-left, lower-right, and upper-right corner points of $S(v)$ in Γ . A \nwarrow -scaling, \swarrow -scaling, \searrow -scaling, \nearrow -scaling of Γ is a \nwarrow -scaling, \swarrow -scaling, \searrow -scaling, \nearrow -scaling of Γ , respectively.



■ **Figure 1** (a) A critical S-node, (b) an almost-bad P-node, (c) a bad P-node, (d) a forbidden P-node, (e) an S-node of Type B, and (f) an S-node of Type C. Yellow, green, and blue regions, represent parallel compositions of any number of S-nodes, at most one critical S-node and any number of non-critical S-nodes, and any number of non-critical S-nodes, respectively.

3 Partial 2-Trees

In this section, we study square-contact representations of partial 2-trees and give the following simple characterization for graphs in this family admitting such representations.

► **Theorem 1.** *Let G be a partial 2-tree. Then, the following statements are equivalent:*

- (i) G is $K_{1,1,3}$ -free,
- (ii) G admits an embedding without separating triangles, and
- (iii) G admits a square-contact representation.

In order to prove [Theorem 1](#), we first show that, without loss of generality, we can restrict our attention to the biconnected partial 2-trees, i.e., the series-parallel graphs.

► **Lemma 1.** *Let G be a $K_{1,1,3}$ -free partial 2-tree. Then, there exists a $K_{1,1,3}$ -free series-parallel graph G^* such that $G \subset G^*$ and G admits a square-contact representation if G^* does.*

Sketch. Let $\beta(H)$ denote the number of blocks, i.e., the maximal biconnected components, of a graph H . Adding to G a new vertex connected to two vertices in $V(G)$ incident to the same cut-vertex of G , belonging to different blocks, and sharing a common face yields a graph G' such that $\beta(G') = \beta(G) - 1$. It is easy to see that G' is $K_{1,1,3}$ -free and that G' does not contain K_4 as a minor. Hence, repeating such an augmentation eventually yields a 2-connected partial 2-tree G^* that is $K_{1,1,3}$ -free. Also, by construction, two vertices in $V(G)$ are adjacent in G^* if and only if they are adjacent in G . Therefore, a square-contact representation of G can be derived from a square-contact representation Γ^* of G^* , by removing from Γ^* all the squares corresponding to vertices in $V(G^*) \setminus V(G)$. ◀

As already observed in [Section 1](#), an embedding without separating triangles is necessary for the existence of a square-contact representation, and $K_{1,1,3}$ has no embedding without separating triangles. Thus, $(iii) \Rightarrow (ii) \Rightarrow (i)$ are immediate. To complete the proof of [Theorem 1](#), we show how to construct a square-contact representation of any $K_{1,1,3}$ -free series-parallel graph, proving that $(i) \Rightarrow (iii)$. We formalize this result in the next theorem.

► **Theorem 2.** *Every $K_{1,1,3}$ -free series-parallel graph admits a square-contact representation.*

Let G be a series-parallel graph and let T be the SPQ-tree of G with respect to any reference edge. We start with some definitions; refer to [Fig. 1](#). Let μ be an S-node in T . We say that μ is *critical*, if $skel_\mu = s-x-t$ and the two children of μ both contain an edge

between their terminals, i.e., $sx, xt \in E(G_\mu)$, and *non-critical*, otherwise. Let μ be a P-node in T containing an edge between its terminals. We say that μ is *almost bad*, if it has exactly one critical child, *bad*, if it has exactly two critical children, and *forbidden*, if it has more than two critical children. Finally, let μ be a P-node in T . We say that μ is *good*, if it is neither bad, nor almost bad, nor forbidden.

We now assign one of three possible types to each S-node μ in T as follows (for each child μ_i of μ , we denote the two terminals of G_{μ_i} as s_i and t_i).

Type A Node μ is of **Type A**, if either $\ell(\mu) > 2$ or $\ell(\mu) = 2$ and at least one child of μ does not contain an edge between its terminals, i.e., $|\{s_1t_1, s_2t_2\} \cap E(G_\mu)| < 2$.

Type B Node μ is of **Type B**, if $\ell(\mu) = 2$, all its children contain an edge between their terminals, and at least one of them is a bad P-node.

Type C Node μ is of **Type C**, if $\ell(\mu) = 2$, and all its children contain an edge between their terminals, and none of them is a bad P-node.

Observe that S-nodes of **Type B** and of **Type C** are also critical.

Let G be a $K_{1,1,3}$ -free series-parallel graph and let T be the SPQ-tree of G with respect to any reference edge. We have the following simple observations regarding the P-nodes in T .

► **Observation 1.** *SPQ-tree T contains no forbidden P-node; refer to Fig. 1(d).*

► **Observation 2.** *Let μ be a P-node in T with terminals s and t such that $st \in E(G_\mu)$. Then, none of the children of μ is of **Type B** and at most two children of μ are of **Type C**.*

We now consider special square-contact representations for the pertinent graphs of the S-nodes in T . Let Γ_μ be a square-contact representation of G_μ . We say that Γ_μ is either an *L-shape*, *pipe*, or *rectangular drawing* of G_μ , if it satisfies the following conditions; refer to Fig. 2.

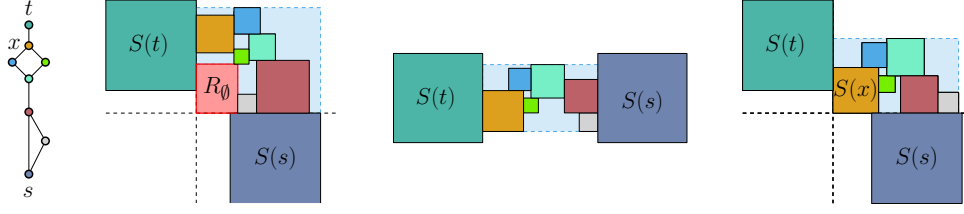
Rectangular drawing $S(t)$ lies to the left and above $S(s)$ and the drawing Γ_μ^- of G_μ^- in Γ_μ lies to the right of $S(t)$ and above $S(s)$; also, all the squares of Γ_μ^- whose left side (bottom side) is collinear with the right side of $S(t)$ (with the top side of $S(s)$) are adjacent to $S(t)$ (to $S(s)$).

L-shape drawing Γ_μ is a rectangular drawing in which there exists a rectangular region (red region R_\emptyset in Fig. 2) inside the bounding box of Γ_μ^- whose interior does not intersect any square in Γ_μ^- and whose lower-left corner lies at the intersection point between the vertical line passing through the right side of $S(t)$ and the horizontal line passing through the top side of $S(s)$.

Pipe drawing $S(t)$ lies to the left of $S(s)$ and the drawing Γ_μ^- of G_μ^- in Γ_μ lies to the right of $S(t)$ and to the left of $S(s)$; also, all the squares of Γ_μ^- whose left side (right side) is collinear with the right side of $S(t)$ (with the left side of $S(s)$) are adjacent to $S(t)$ (to $S(s)$).

In the following, we generally refer to a drawing of an S-node μ in T (of G_μ) which is either an L-shape drawing, a pipe drawing, or a rectangular drawing as a *valid drawing* of μ (of G_μ).

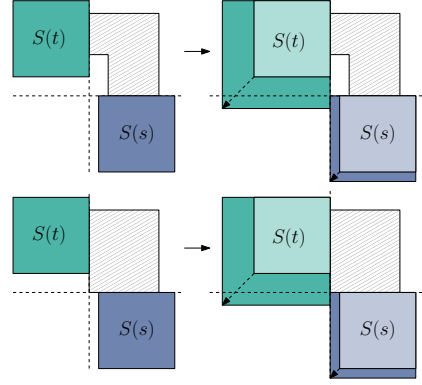
Let Γ_μ^- be the square-contact representation of G_μ^- contained in Γ_μ . Observe that Γ_μ^- lies in the interior of an orthogonal hexagon with an internal angle equal to 270° , i.e., an *L-shape polygon* (or, simply, *L-shape*), if Γ_μ^- is an L-shape drawing. Also, Γ_μ^- lies in the interior of a rectangle whose opposite vertical sides are adjacent to the right side of $S(t)$ and to the left side of $S(s)$, i.e., a *horizontal pipe*, if Γ_μ^- is a pipe drawing. Finally, Γ_μ^- lies in the interior of a rectangle whose left and bottom side are adjacent to the right side of $S(t)$ and to the top side of $S(s)$, respectively, if Γ_μ^- is a rectangular drawing.



■ **Figure 2** From left to right: pertinent G_μ of an S-node μ with terminals s and t , L-shape and pipe drawings of G_μ , respectively, and a rectangular drawing of an S-node ν with pertinent $G_\nu = G_\mu \cup sx$. The L-shape region and horizontal pipe enclosing G_μ^- and the rectangle enclosing G_ν^- are shaded blue.

Proof of Theorem 2. In order to prove Theorem 2, we proceed as follows. Let G be a $K_{1,1,3}$ -free series-parallel graph and let T be the SPQ-tree of G rooted at a Q-node ρ with terminals s and t , whose unique child τ is an S-node. Observe that such a Q-node always exists, since G is simple, and that node τ is either of **Type A** or of **Type C**, since G is $K_{1,1,3}$ -tree. We perform a bottom-up traversal in T to construct one or two valid drawings of G_μ , for each S-node $\mu \in T$. Namely, we compute:

- an L-shape drawing, if μ is of **Type A** (Lemma 4),
- a pipe drawing, if μ is of **Type B** (Lemma 5), and
- both a pipe drawing and a rectangular drawing, if μ is of **Type C** (Lemma 6).



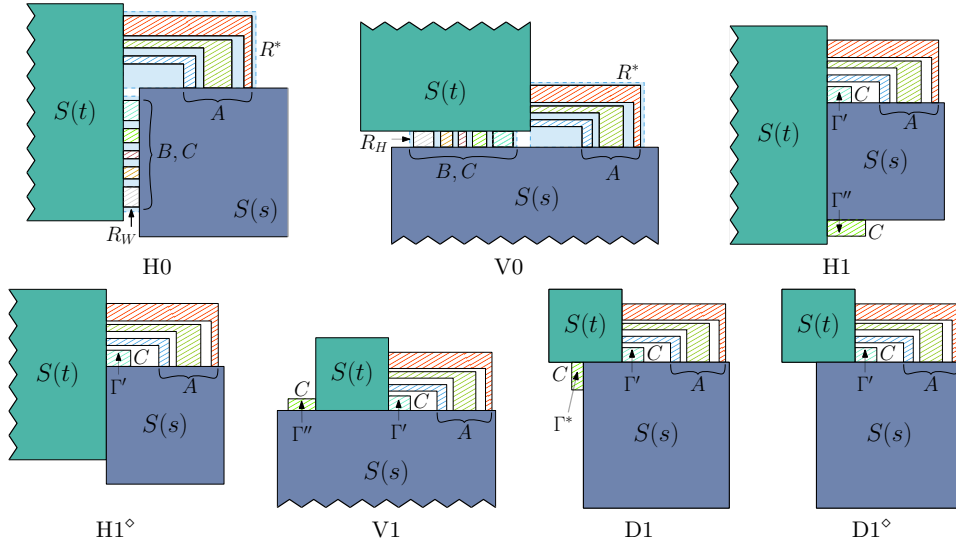
■ **Figure 3** Transforming Γ_τ into Γ_ρ .

Thus, when node τ is considered, we can compute either an L-shape drawing of G_τ , if τ is of **Type A**, or a rectangular drawing of G_τ , if τ is of **Type C**. Further, both such valid drawings Γ_τ of G_τ can be easily turned into a square-contact representation Γ_ρ of $G = G_\tau \cup st$, by performing a \hat{t} -scaling and an \hat{s} -scaling of Γ_τ in such a way that the right side of $S(t)$ and the left side of $S(s)$ touch; refer to Fig. 3. This is possible since both in an L-shape drawing and in a rectangular drawing of G_τ all the squares of G_τ^- whose left side (bottom side) is collinear with the right side of $S(t)$ (with the top side of $S(s)$) are adjacent to $S(t)$ (to $S(s)$).

Let μ be an S-node and let μ_1, \dots, μ_k be the children of μ in T . If each child μ_i of μ is a Q-node, then node μ is of **Type A**, if $\ell(\mu) > 2$, and it is of **Type C**, otherwise. It is not difficult to see that, in the former case, G_μ admits an L-shape drawing and that, in the latter case, G_μ admits both a pipe drawing and a rectangular drawing. In the remainder of the section, we consider the case in which μ has both Q-node and P-node children.

We first show how to construct special square-contact representations of G_μ , that we call *canonical drawings*, for any P-node μ in T , assuming that valid drawings have been computed for each S-node child of μ . We distinguish five possible canonical drawings, depending on **1.** the number and type of the S-node children of μ and **2.** the presence of edge st . Each canonical drawing has three variants: **vertical (V)**, **horizontal (H)**, and **diagonal (D)**. We name such canonical representations XY drawings, where $X \in \{V, H, D\}$ denotes the variant of the representation and $Y = 1$, if $st \in E(G_\mu)$, and $Y = 0$, otherwise. Canonical drawings share the following main property (which, in fact, also holds for valid drawings).

► **Property 1.** Let Γ_μ be a valid drawing or a canonical drawing of G_μ . Then, for each vertex v in $V(G_\mu^-)$, it holds that $vs \in E(G_\mu)$ ($vt \in E(G_\mu)$) if:



■ **Figure 4** Canonical drawings of a P-node μ . The striped regions correspond to L-shapes, horizontal pipes, and rectangles enclosing the square-contact representations of graphs $G_{\mu_i}^-$, for each S-node child μ_i of μ . Labels A , B , and C indicate the type of each S-node.

1. $S(v)$ has a side that is collinear with a side of $S(s)$ (of $S(t)$) in Γ_μ and
2. $S(v)$ is separated from $S(s)$ (from $S(t)$) in Γ_μ by the line passing through such a side.

Property 1 allows us to modify canonical and valid drawings by appropriate \hat{s} -scaling and \hat{t} -scaling transformations, with $\circ \in \{\nwarrow, \nearrow, \searrow, \swarrow\}$, preserving adjacencies between vertices in G_μ .

First, consider a P-node μ in T with terminals s and t such that $st \notin E(G_\mu)$ and let μ_1, \dots, μ_k be the S-node children of μ . We say that a square-contact representation Γ_μ of G_μ is an *H0 drawing* or a *V0 drawing*, if it satisfies the following conditions (in addition to **Property 1**); refer to **Fig. 4**.

H0 drawing $S(t)$ lies to the left of $S(s)$, the bottom side of $S(s)$ lies below the bottom side of $S(t)$, and the drawing of G_μ^- in Γ_μ lies to the right of $S(t)$, below the top side of $S(t)$, above the bottom side of $S(s)$, and to the left of the right side of $S(s)$.

V0 drawing $S(t)$ lies above $S(s)$, the left side of $S(s)$ lies to the right of the left side of $S(t)$, and the drawing of G_μ^- in Γ_μ lies above $S(s)$, to the right of the left side of $S(s)$, below the top side of $S(t)$, and to the left of the right side of $S(s)$.

Now, consider a P-node μ in T with terminals s and t such that $st \in E(G_\mu)$ and let μ_1, \dots, μ_k be the S-node children of μ . We say that a square-contact representation Γ_μ of G_μ is an *H1 drawing*, an *H1° drawing*, a *V1 drawing*, a *D1 drawing*, or a *D1° drawing*, if it satisfies the following conditions (in addition to **Property 1**); refer to **Fig. 4**.

H1 drawing $S(t)$ lies to the left of $S(s)$, the bottom side of $S(s)$ lies above the bottom side of $S(t)$, and the drawing of G_μ^- in Γ_μ lies to the right of $S(t)$, below the top side of $S(t)$, above the bottom side of $S(s)$, and to the left of the right side of $S(s)$.

H1° drawing $S(t)$ lies to the left of $S(s)$, the bottom side of $S(s)$ lies below the bottom side of $S(t)$, and the drawing of G_μ^- in Γ_μ lies to the right of $S(t)$, below the top side of $S(t)$, above the top side of $S(s)$, and to the left of the right side of $S(s)$.

- V1 drawing** $S(t)$ lies above $S(s)$ and the drawing of G_μ^- in Γ_μ lies above $S(s)$, below the top side of $S(t)$, to the right of the left side of $S(s)$, and to the left of the right side of $S(s)$.
- D1 drawing** $S(t)$ lies above $S(s)$ and the left side of $S(t)$ lies to the left of the left side of $S(s)$, and the drawing of G_μ^- in Γ_μ lies to the right of the left side of $S(t)$, below the top side of $S(t)$, above the bottom side of $S(s)$, and to the left of the right side of $S(s)$.
- D1 $^\diamond$ drawing** Γ_μ is a D1 drawing of G_μ in which the drawing of G_μ^- lies to the right of $S(t)$.

We now present two lemmata for the possible canonical drawings of each P-node μ in T . Recall that, by [Observation 1](#), we can assume that μ is not a forbidden P-node. Let μ_1, \dots, μ_k be the S-node children of μ . The general strategy in the proofs of both lemmata consists of **1.** computing appropriate valid drawings $\Gamma_{\mu_1}, \dots, \Gamma_{\mu_k}$ for the pertinent graphs $G_{\mu_1}, \dots, G_{\mu_k}$ of μ_1, \dots, μ_k , respectively, **2.** modifying the square-contact representation of $G_{\mu_i}^-$ contained in Γ_{μ_i} , for $i = 1, \dots, k$, by means of affine transformations, so that representations derived from S-nodes of the same type lie in the interior of the same polygon, and finally **3.** composing the resulting drawings into a canonical drawing of G_μ ; refer to [Appendix B.1](#).

We first consider the case in which μ does not contain an edge between its terminals. In this case, by [Lemmata 4, 5, and 6](#), we can assume that Γ_{μ_i} is an L-shape drawing, if μ_i is of **Type A**, and a pipe drawing, if μ_i is of **Type B** or of **Type C**, for $i = 1, \dots, k$.

► **Lemma 2.** *Let μ be a P-node in T with terminals s and t such that $st \notin E(G_\mu)$. Then, graph G_μ admits an H0 drawing and a V0 drawing.*

Then, we consider the case in which μ contains an edge between its terminals. Recall that, by [Observation 2](#), node μ has no child of **Type B** and at most two children of **Type C**. In particular, node μ has two children of **Type C**, if it is bad, and one child of **Type C**, if it is almost bad. In this case, by [Lemmata 4 and 6](#), we can assume that Γ_{μ_i} is an L-shape drawing, if μ_i is of **Type A**, and a rectangular drawing, if μ_i is of **Type C**, for $i = 1, \dots, k$.

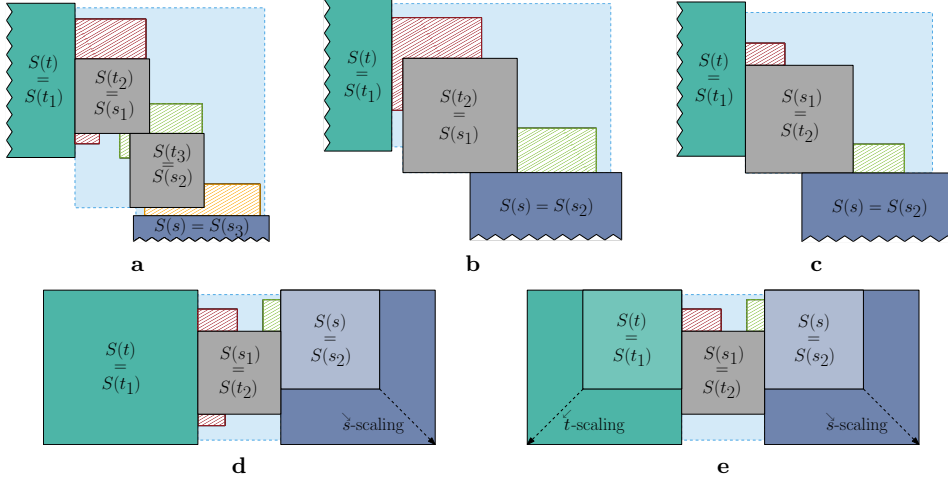
► **Lemma 3.** *Let μ be a P-node in T with terminals s and t such that $st \in E(G_\mu)$. Then, graph G_μ admits*

- an H1 drawing, a V1 drawing, and a D1 drawing, if μ is bad, or
- an H1 $^\diamond$ drawing and a D1 $^\diamond$ drawing, if μ is good or almost bad.

We finally turn our attention to the valid drawings of the S-nodes in T . Let μ be an S-node in T and let μ_1, \dots, μ_k be the children of μ (where the virtual edge e_i , corresponding to node μ_i , precedes the virtual edge e_{i+1} , corresponding to node μ_{i+1} , from t to s in $skel_\mu$). The next three lemmata immediately imply [Theorem 2](#). To simplify their proofs, we assume that each child of μ is a P-node. In fact, the case in which a child of μ is a Q-node can be treated analogously to that of a P-node containing an edge between its terminals. The general strategy in the proofs of all three lemmata consists of **1.** computing appropriate canonical drawings $\Gamma_{\mu_1}, \dots, \Gamma_{\mu_k}$ for the pertinent graphs $G_{\mu_1}, \dots, G_{\mu_k}$ of μ_1, \dots, μ_k , respectively, **2.** modifying these drawings, by means of affine transformations, so that the squares corresponding to terminals shared by different children of μ can be identified without introducing any overlapping between squares corresponding to internal vertices of G_{μ_i} and G_{μ_j} , with $i \neq j$, and finally **3.** composing the resulting drawings into a valid drawing of G_μ .

► **Lemma 4.** *If μ is an S-node of **Type A**, then G_μ admits an L-shape drawing.*

Proof. We first describe how to select a valid drawing of Γ_{μ_i} of G_{μ_i} , for $i = 1, \dots, k$, based on whether (i) $\ell(\mu) > 2$ or (ii) $\ell(\mu) = 2$. Recall that, if $\ell(\mu) = 2$, then at least one child of μ does not contain an edge between its terminals, say μ_1 (the case in which $s_1 t_1 \in E(G_{\mu_1})$ and $s_2 t_2 \notin E(G_{\mu_2})$ is analogous).



■ **Figure 5** Illustrations for the proofs of [Lemmata 4, 5, and 6](#). Striped polygons of the same color enclose different parts of the drawing of each graph $G_{\mu_i}^-$ (contained in the canonical drawing Γ_{μ_i} of G_{μ_i}). (a) An H1 drawing of G_{μ_1} , a D1 drawing of G_{μ_2} , and a $D1^\diamond$ drawing of G_{μ_3} are combined into an L-shape drawing. (b) An H0 drawing of G_{μ_1} and a $D1^\diamond$ drawing of G_{μ_2} are combined into an L-shape drawing. (c) An $H1^\diamond$ drawing of G_{μ_1} and a $D1^\diamond$ drawing of G_{μ_2} are combined into a rectangular drawing. (d) An H1 drawing of G_{μ_1} and a $D1^\diamond$ drawing of G_{μ_2} are combined into a pipe drawing. (e) An $H1^\diamond$ drawing of G_{μ_1} and a $D1^\diamond$ drawing of G_{μ_2} are combined into a pipe drawing.

- (i) By [Lemma 2](#) and [Lemma 3](#), we can construct a drawing Γ_{μ_i} , for each μ_i , such that:
 - a. Γ_{μ_1} is an H0 drawing, if $s_1 t_1 \notin E(G_{\mu_1})$, and Γ_{μ_1} is an H1 drawing ($H1^\diamond$ drawing), if μ_1 is bad (if μ_1 is good or almost bad);
 - b. Γ_{μ_2} is a V0 drawing, if $s_2 t_2 \notin E(G_{\mu_2})$, and Γ_{μ_2} is a D1 drawing ($D1^\diamond$ drawing), if μ_2 is bad (if μ_2 is good or almost bad);
 - c. Γ_{μ_i} is a V0 drawing, if $s_i t_i \notin E(G_{\mu_i})$, and Γ_{μ_i} is a V1 drawing ($D1^\diamond$ drawing), if μ_i is bad (if μ_i is good or almost bad), for every $i > 2$.
- (ii) By [Lemma 2](#) and [Lemma 3](#), we can construct an H0 drawing Γ_{μ_1} of G_{μ_1} and a V1 drawing ($D1^\diamond$ drawing) Γ_{μ_2} of G_{μ_2} , if μ_2 is bad (if μ_2 is good or almost bad).

We show how to compose all such drawings into an L-shape drawing Γ_μ of G_μ as follows. Refer to [Fig. 5\(a\)](#) for an example of how to compose drawings Γ_{μ_i} , with $i = 1, \dots, k$, in case (i) and to [Fig. 5\(b\)](#) for an example of how to compose drawings Γ_{μ_1} and Γ_{μ_2} in case (ii). First, we scale $S(s_i)$ and $S(t_i)$ in Γ_{μ_i} so that the bounding box of the drawing of each connected component of $G_{\mu_i} - \{s_i, t_i\}$ in Γ_{μ_i} , for $i = 1, \dots, k$, becomes arbitrarily small with respect to the drawing of $S(s_i)$ and $S(t_i)$. This avoids overlapping between internal vertices of G_{μ_i} and G_{μ_j} , with $i \neq j$, in the next phases of the construction. Then, we scale and translate each drawing Γ_{μ_i} so that $S(t_{i+1}) = S(s_i)$, with $i < k$. It is easy to see that, by the choice of the canonical drawings of each G_{μ_i} , there exists a rectangular region in Γ_μ whose interior does not intersect any square representing a vertex in G_μ^- and whose lower-left corner lies at the intersection point between the vertical line passing through the right side of $S(t)$ and the horizontal line passing through the top side of $S(s)$ in Γ_μ . ◀

The proof of the next two lemmata also exploits rotations of drawings Γ_{μ_i} and can be carried out in a fashion similar to the proof of [Lemma 4](#). Refer to [Appendix B.1](#).

► **Lemma 5.** *If μ is an S-node of Type B, then G_μ admits a pipe drawing.*

► **Lemma 6.** *If μ is an S-node of Type C, then G_μ admits a pipe and a rectangular drawing.*

4 Triconnected Simply-Nested Graphs

In this section, we devote our attention to 3-connected simply-nested graphs.

A cycle-tree with a single edge removed from the outer cycle is a *path-tree* (to avoid special cases, we allow the outer cycle of the cycle-tree to be a 2-gon). In path-trees, we refer to vertices in the tree as *tree vertices* and vertices in the external path as *path vertices*. A tree vertex can *see* a path vertex if they share a face in the original cycle-tree. Define an *almost-triconnected path-tree with root ρ , leftmost path vertex ℓ , and rightmost path vertex r* to be a path-tree containing in one of its faces a tree vertex ρ and path vertices ℓ and r such that if the edges $\rho\ell$, ρr , and ℓr were added, the resulting graph would be a 3-connected cycle-tree.

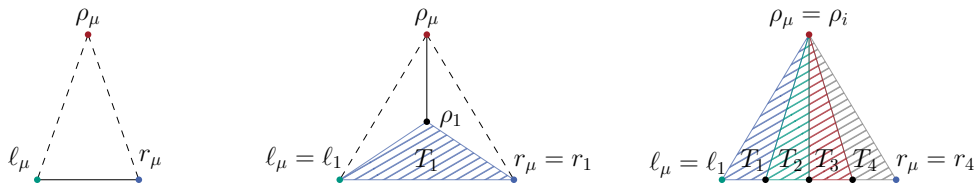
SPQ-decomposition of path-trees. We now describe a recursive decomposition for almost-triconnected path-trees. We call this an SPQ-decomposition, because it bears a striking similarity to the SPQ-decomposition of series-parallel graphs. Let G be a 3-connected cycle-tree, let ℓr be an edge incident to the outer cycle of G , and let ρ be a tree vertex incident to the internal face of G edge ℓr is incident to. Also, let $G' = G - \ell r$ be the almost-triconnected path-tree obtained from G by removing edge ℓr . Graph G' defines a rooted decomposition tree T whose nodes are of three different kinds: *S*-, *P*-, and *Q*-nodes. Each node μ of T is associated with a path-tree G_μ with root ρ_μ , leftmost path vertex ℓ_μ , and rightmost path vertex r_μ obtained—except the *Q*-nodes—from smaller path-trees T_i with root ρ_i , leftmost path vertex ℓ_i , and rightmost path vertex r_i , for $i = 1, \dots, k$, as follows.

- A *Q*-node μ is associated with a path-tree G_μ with three vertices: one tree vertex ρ_μ and two path vertices ℓ_μ and r_μ . The tree vertex ρ_μ is the root of G_μ , while path vertices ℓ_μ and r_μ are the leftmost and the rightmost path vertex of G_μ , respectively. Edge $\ell_\mu r_\mu$ will always exist, but edges $\rho_\mu \ell_\mu$ and $\rho_\mu r_\mu$ may or may not exist; see Fig. 6(left).
- An *S*-node μ is associated with a path-tree G_μ obtained from path-tree T_1 by adding a new root ρ_μ connected to ρ_1 . Also, $\ell_\mu = \ell_1$ and $r_\mu = r_1$ are the leftmost and the rightmost path vertex of G_μ , respectively. Edges $\rho_\mu \ell_\mu$ and $\rho_\mu r_\mu$ may or may not exist; see Fig. 6(middle).
- A *P*-node μ is associated with a path-tree G_μ obtained from path-trees T_i by merging T_1, T_2, \dots, T_k from left to right as follows. First, roots ρ_i are identified into a new root ρ_μ . Then, the rightmost path vertex r_i of T_i and the leftmost path vertex ℓ_{i+1} of T_{i+1} are identified, for $i = 1, \dots, k-1$. Path vertices $\ell_\mu = \ell_1$ and $r_\mu = r_k$ are the leftmost and the rightmost path vertex of G_μ , respectively; see Fig. 6(right).

We have the following lemma.

► **Lemma 7.** *Any almost-triconnected path-tree admits an SPQ-decomposition.*

In Appendix B.2 we show how to construct a square-contact representation of any almost-triconnected path-tree G without separating triangles and whose outer face is not a triangle

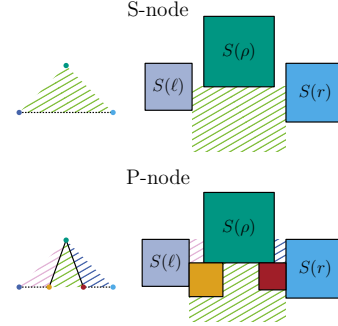


■ **Figure 6** Path-trees associated with a *Q*-node (left), an *S*-node (middle), and a *P*-node (right). Dashed edges may or may not exist.

by inductively maintaining the invariant depicted in Fig. 7 for the S- and P-nodes of an SQP-decomposition of G . We formalize this result in the next lemma.

► **Lemma 8.** *Any almost-triconnected path-tree G without separating triangles and whose outer face is not a triangle admits a square-contact representation.*

To construct a square-contact representation for a 3-connected cycle-tree, it is natural to remove an edge in the outer cycle to obtain a path-tree, use Lemma 8 to construct a square-contact representation, and then attempt to reintroduce a contact for the removed edge. However, because Lemma 8 places the leftmost and rightmost path vertices on the left and right side of the drawing, it is unclear how to add a contact between them. Instead, we split the cycle-tree into two overlapping almost-triconnected path-trees, obtain their square-contact representations by Lemma 7, and overlay them to form a square-contact representation for the entire cycle-tree.



► **Figure 7** Invariants for S- and P-nodes with more than two path vertices.

► **Theorem 3.** *Any 3-connected cycle-tree G without separating triangles and whose outer face is not a triangle admits a square-contact representation.*

As Halin graphs are 3-connected cycle-trees without separating triangles and have, except for K_4 , a non-triangular outer face, we have the following.

► **Corollary 4.** *Any Halin graph $G \not\cong K_4$ admits a square-contact representation.*

Next, we investigate square-contact representations of 2-outerplanar simply-nested graphs that are not cycle-trees (Theorem 5) and 3-outerplanar simply nested graphs (Theorem 6).

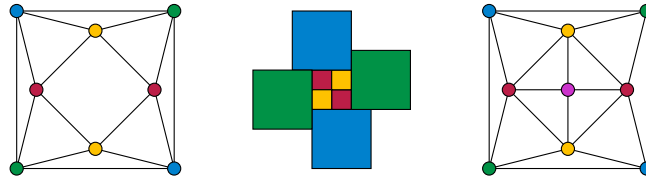
► **Theorem 5.** *There exists a 3-connected 2-outerplanar simply-nested graph that does not admit any proper square-contact representation.*

Proof. Consider the two nested quadrilaterals shown in Fig. 8(left). One of its two quadrilateral faces must be the outer one, giving the embedding shown. In any square-contact representation, the inner polygon surrounded by the squares for the four outer vertices must be a rectangle, as it has only four sides. Each of the four inner squares must touch one of the four corners of this rectangle (the corner made by its two outer neighbors). For the four inner squares to touch the four corners of the rectangle and each other, the only possibility is that the rectangle is a square and each inner square fills one quarter of it, as shown in Fig. 8(middle). However, this representation is improper, as diagonally-opposite inner squares meet at their corners. ◀

► **Theorem 6.** *There exists a 3-connected 3-outerplanar simply-nested graph that does not admit any square-contact representation.*

Proof. Consider the graph shown in Fig. 8(right). Its quadrilateral face must be the outer one, giving the embedding shown. As in the proof of Theorem 5, the only possible representation for its two outer quadrilaterals has the four outer squares surrounding a central square region, divided into four quarters representing the four middle vertices, as shown in Fig. 8(middle). However, this representation leaves no room for the inner vertex. ◀

We remark that the graph of Theorem 6 is actually 2-outerplanar simply-nested, but not with its quadrilateral face as the outer face.



■ **Figure 8** Left: Two nested quadrilaterals form a graph with no proper square-contact representation. Middle: An improper square-contact representation for the same graph. Right: A graph with no square-contact representation, even an improper one.

5 Conclusions

In this paper, we provided simple characterizations for two notable families of planar graphs that admit proper square-contact representations. Moreover, we introduced a new decomposition for an interesting family of polyhedral graphs that generalize the Halin graphs, i.e., the 3-connected cycle-trees. Finally, we showed that the absence of separating triangles and a non-triangular outer face do not guarantee the existence of weak and proper square-contact representations of 3-outerplanar and 2-outerplanar simply-nested graphs, respectively.

Acknowledgements. We thank Jawaherul M. Alam for useful discussions on this subject.

References

- 1 M. J. Alam, D. Eppstein, M. Kaufmann, S. G. Kobourov, S. Pupyrev, A. Schulz, and T. Ueckerdt. Contact graphs of circular arcs. In F. Dehne, J. Sack, and U. Stege, editors, *WADS '15*, volume 9214 of *LNCS*, pages 1–13. Springer, 2015.
- 2 C. Bowen, S. Durocher, M. Löffler, A. Rounds, A. Schulz, and C. D. Tóth. Realization of simply connected polygonal linkages and recognition of unit disk contact trees. In E. D. Giacomo and A. Lubiw, editors, *GD '15*, volume 9411 of *LNCS*, pages 447–459. Springer, 2015.
- 3 S. Chaplick, S. G. Kobourov, and T. Ueckerdt. Equilateral l-contact graphs. In A. Brandstädt, K. Jansen, and R. Reischuk, editors, *WG '13*, volume 8165 of *LNCS*, pages 139–151. Springer, 2013.
- 4 R. J. Cimikowski. Finding hamiltonian cycles in certain planar graphs. *Inf. Process. Lett.*, 35(5):249–254, 1990.
- 5 G. Di Battista, P. Eades, R. Tamassia, and I. G. Tollis. *Graph Drawing: Algorithms for the Visualization of Graphs*. Prentice-Hall, 1999.
- 6 S. Felsner and M. C. Francis. Contact representations of planar graphs with cubes. In F. Hurtado and M. J. van Kreveld, editors, *SoCG '11*, pages 315–320. ACM, 2011.
- 7 D. Gonçalves, B. Lévêque, and A. Pinlou. Triangle contact representations and duality. *Discrete Comput. Geom.*, 48(1):239–254, 2012.
- 8 H. Harborth. Lösung zu Problem 664A. *Elemente der Mathematik*, 29:14–15, 1974.
- 9 P. Hliněný. Contact graphs of line segments are NP-complete. *Discrete Math.*, 235(1-3):95–106, 2001.
- 10 O. Schramm. *Combinatorially Prescribed Packings and Applications to Conformal and Quasiconformal Maps*. PhD thesis, Princeton University, 1990.
- 11 O. Schramm. Square tilings with prescribed combinatorics. *Israel J. Math.*, 84(1-2):97–118, 1993.
- 12 K. Stephenson. *Introduction to Circle Packing: The theory of discrete analytic functions*. Cambridge University Press (1), 2005.

A Omitted Definitions

A graph is *connected* if it contains a path between any two vertices. A *cutvertex* is a vertex whose removal disconnects the graph. A *separation pair* is a pair of vertices whose removal disconnects the graph. A connected graph is *2-connected* if it does not have a cutvertex and a 2-connected graph is *3-connected* if it does not have a separation pair. The maximal 2-connected components of a graphs are its *blocks*.

A graph is *planar* if it admits a drawing in the plane without edge crossings. A *combinatorial embedding* is an equivalence class of planar drawings, where two drawings of a graph are *equivalent* if they determine the same circular orderings for the edges around each vertex. A planar drawing partitions the plane into topologically connected regions, called *faces*. The bounded faces are the *inner faces*, while the unbounded face is the *outer face*. A combinatorial embedding together with a choice for the outer face defines a *planar embedding*. An *embedded graph* (*plane graph*) is a planar graph with a fixed combinatorial embedding (fixed planar embedding).

B Omitted Proofs

In this appendix, we give full details of omitted or sketched proofs.

B.1 Omitted Proofs of Section 3

► **Lemma 1.** *Let G be a $K_{1,1,3}$ -free partial 2-tree. Then, there exists a $K_{1,1,3}$ -free series-parallel graph G^* such that $G \subset G^*$ and G admits a square-contact representation if G^* does.*

Proof. Let $\beta(H)$ denote the number of blocks of a graph H . We show that G can be augmented to a $K_{1,1,3}$ -free partial 2-tree G' such that $\beta(G') = \beta(G) - 1$, by adding to G a new vertex connected to two vertices in $V(G)$ incident to the same cut-vertex of G , belonging to different blocks, and sharing a common face. Hence, repeating such an augmentation eventually yields a 2-connected partial 2-tree G^* that is $K_{1,1,3}$ -free. Also, by construction, two vertices in $V(G)$ are adjacent in G^* if and only if they are adjacent in G . Therefore, a square-contact representation of G can be derived from a square-contact representation Γ^* of G^* , by removing from Γ^* all the squares corresponding to vertices in $V(G^*) \setminus V(G)$.

Suppose that $\beta(G) > 1$, as otherwise G is 2-connected and we can set $G^* = G$. Consider a planar embedding \mathcal{E} of G and a cut-vertex c of G . Let $e_1 = (c, u)$ and $e_2 = (c, v)$ be two edges incident to c such that (i) e_1 and e_2 belong to distinct blocks B_1 and B_2 of G , respectively, and (ii) e_1 precedes e_2 in the clockwise order of the edges incident to c in \mathcal{E} . Let f be the face of \mathcal{E} that lies to the right of e_1 (to the left of e_2) when traversing e_1 (e_2) from c to u (from c to v). Augment G to graph G' by adding a new vertex w and edges $e'_1 = (w, u)$ and $e'_2 = (w, v)$ inside f . Clearly, blocks B_1 and B_2 of G are now “merged” in a single block B in G' . Also, G' is a partial 2-tree. In fact, since G is a partial 2-tree and since any path connecting a vertex in $V(B_1)$ and a vertex in $V(B_2)$ must pass either through c or through w , graph G' does not contain K_4 as a minor. Finally, G' is $K_{1,1,3}$ -free. This is due to the fact that G is $K_{1,1,3}$ -free and that, since u and v belong to different blocks of G , these vertices do not belong to an induced $K_{1,1,2}$ subgraph of G . ◀

► **Lemma 2.** *Let μ be a P -node in T with terminals s and t such that $st \notin E(G_\mu)$. Then, graph G_μ admits an $H0$ drawing and a $V0$ drawing.*

Proof. In order to obtain an H0 drawing Γ_{H0} of G_μ (a V0 drawing Γ_{V0} of G_μ) we compose the drawings Γ_{μ_i} of G_{μ_i} , with $1 \leq i \leq k$, as depicted in Fig. 4(H0) (in Fig. 4(V0)). Specifically, we proceed as follows. First, we scale all the pipe drawings of the children of μ of **Type B** and of **Type C** in such a way that they have the same width W (the same height H). Then, we compose these drawings in such a way for them to fit in a rectangle R_W of width W (a rectangle R_H of height H) and such that no two pipes overlap; let Γ_P be the resulting drawing. Similarly, we scale all the L-shape drawings of the children of μ of **Type A** in such a way that they fit into a rectangle R^* , the left side of each L-shape is incident to the left side of R^* , the bottom side of each L-shape is incident to the bottom side of R^* , and no two L-shapes overlap; let Γ_L be the resulting drawing. Then, we draw u and v as squares $S(u)$ and $S(v)$ of appropriate size in Γ_{H0} (in Γ_{V0}) in such a way that $S(t)$ is incident to the left side of R_W (top side of R_H), $S(s)$ is incident to the right side of R_W (bottom side of R_H). Finally, we insert a scaled copy of Γ_L in Γ_{H0} (in Γ_{V0}) such that the left side of each L-shape contained in Γ_L is adjacent to the right side of $S(t)$ and the bottom side of each L-shape contained in Γ_L is adjacent to the top side of $S(s)$. This concludes the construction of Γ_{H0} and of Γ_{V0} . \blacktriangleleft

► **Lemma 3.** *Let μ be a P-node in T with terminals s and t such that $st \in E(G_\mu)$. Then, graph G_μ admits*

- an H1 drawing, a V1 drawing, and a D1 drawing, if μ is bad, or
- an $H1^\circ$ drawing and a $D1^\circ$ drawing, if μ is good or almost bad.

Proof. We define rectangle R^* and the drawing Γ_L enclosing the drawing of $G_{\mu_i}^-$ in the L-shape drawing Γ_{μ_i} of each child μ_i of μ of **Type A** exactly as in the proof of Lemma 2.

We prove the first part of the statement. Let μ_1 and μ_2 be the two S-node children of μ of **Type C** and let Γ_{μ_1} and Γ_{μ_2} be rectangular drawings of G_{μ_1} and G_{μ_2} , respectively. We show how to construct an H1 drawing Γ_{H1} of G_μ . The construction of a V1 drawing being symmetric. Refer to Figs. 4(H1) and 4(V1). First, we draw u and v as squares $S(u)$ and $S(v)$ of appropriate size such that $S(t)$ lies to the left of $S(s)$, the bottom side of $S(s)$ lies above the bottom side of $S(t)$, the top side of $S(s)$ lies below the top side of $S(t)$, and the right side of $S(t)$ is adjacent to the left side of $S(s)$; let Γ_H be the resulting drawing. Then, we insert a scaled copy of Γ_L in Γ_H such that the left side of each L-shape contained in Γ_L is adjacent to the right side of $S(t)$ and the bottom side of each L-shape contained in Γ_L is adjacent to the top side of $S(s)$. We obtain Γ_{H1} from Γ_H as follows. First, we insert a scaled copy Γ' of $G_{\mu_1}^-$ in Γ_{μ_1} in the interior of Γ_L in such a way that the left side and the bottom side of the rectangle enclosing Γ' is adjacent to the right side of $S(t)$ and to the top side of $S(s)$, respectively, and Γ' does not overlap with any square in Γ_L . Finally, consider the drawing Γ'' of $G_{\mu_2}^-$ in Γ_{μ_2} after being mirrored with respect to the x -axis. We insert a scaled copy of Γ'' in Γ_H in such a way that the top side and the left side of the rectangle enclosing Γ'' is adjacent to the right side of $S(s)$ and to the bottom side of $S(t)$, respectively. Observe that the flip of the drawing of $G_{\mu_2}^-$ with respect to the x -axis has been performed to preserve adjacencies in the final drawing, as we are placing Γ'' below $S(s)$. We now show how to construct a D1 drawing Γ_{D1} of G_μ . Refer to Fig. 4(D1). First, we draw u and v as squares $S(u)$ and $S(v)$ of appropriate size such that $S(t)$ lies above $S(s)$, the left side of $S(t)$ lies to the left of the left side of $S(s)$, the right side of $S(t)$ lies between the left and the right side of $S(s)$, and the bottom side of $S(t)$ is adjacent to the top side of $S(s)$; let Γ_D be the resulting drawing. Then, we extend Γ_D by inserting in it a scaled copy of Γ_L and a scaled copy Γ' of $G_{\mu_1}^-$ in Γ_{μ_1} as discussed above for constructing an H1 drawing. Observe that Γ_D is now a $D1^\circ$ drawing. Finally, consider the drawing Γ^* of $G_{\mu_2}^-$ in Γ_{μ_2} after being mirrored

with respect to the y -axis and rotated by -90° . We insert a scaled copy of Γ^* in Γ_D in such a way that the top side and the right side of the rectangle enclosing Γ^* is adjacent to the bottom side of $S(t)$ and to the left side of $S(s)$, respectively. Observe that the flip of the drawing of $G_{\mu_2}^-$ with respect to the y -axis and the counter-clockwise rotation by 90° have been performed to preserve adjacencies in the final drawing, as we are placing Γ^* below $S(t)$ and to the left of $S(s)$.

Now, we prove the second part of the statement. Observe that, since μ is good or almost bad, it has at most one S-node child of **Type C**, as S-nodes of **Type C** are critical. For the construction of an $H1^\circ$ drawing and of a $D1^\circ$ drawing we proceed as discussed above for the construction of Γ_{H1} and of Γ_{D1} , respectively. However, in this case, we can simply omit the last step in these constructions, in which we extend Γ_{H1} and Γ_{D1} with drawings Γ'' and Γ^* , respectively. As observed above, the construction of Γ_{D1} immediately yields a $D1^\circ$ drawing, if μ is good or almost bad. Refer to Fig. 4(D1 $^\circ$). Instead, in order to obtain an $H1^\circ$ drawing from Γ_{H1} , we only need to perform a final negative \hat{t} -scaling of Γ_{H1} so that the bottom side of $S(t)$ lies above the bottom side of $S(s)$. Refer to Fig. 4(H1 $^\circ$). This concludes the proof. ◀

► **Lemma 5.** *If μ is an S-node of **Type B**, then G_μ admits a pipe drawing.*

Proof. Recall that $\ell(\mu) = 2$, at least one of the children of μ is a bad P-node, say μ_1 , and the other child contains an edge between its terminals. The case in which μ_2 is bad and μ_1 is not bad and contains an edge between its terminals can be treated symmetrically.

By Lemma 3, we can construct a drawing Γ_{μ_1} of G_{μ_1} and a drawing Γ_{μ_2} of G_{μ_2} such that Γ_{μ_1} is an $H1$ drawing and Γ_{μ_2} is a $V1$ drawing, if μ_2 is also bad, or a $D1^\circ$ drawing, if μ_2 is good or almost bad.

We show how to compose Γ_{μ_1} and Γ_{μ_2} into a pipe drawing of G_μ as follows. Refer to Fig. 5(d) for an example where Γ_{μ_1} is an $H1$ drawing and Γ_{μ_2} is a $D1^\circ$ drawing. First, we replace Γ_{μ_2} with its copy rotated by -90° . Second, we scale $S(s_i)$ and $S(t_i)$ in Γ_{μ_i} so that the bounding box of the drawing of each connected component of $G_{\mu_i} - \{s_i, t_i\}$ in Γ_{μ_i} , with $i \in \{1, 2\}$, becomes arbitrarily small with respect to the drawing of $S(s_i)$ and $S(t_i)$. Third, we scale and translate drawing Γ_{μ_1} and Γ_{μ_2} so that $S(t_2) = S(s_1)$. Finally, we perform an \hat{s} -scaling of the obtained drawing of G_μ so that the drawing of G_μ^- lies above the bottom side of $S(s)$. By construction and by the choice of the canonical drawings of G_{μ_1} and G_{μ_2} , the resulting drawing of G_μ is a pipe drawing. This concludes the proof. ◀

► **Lemma 6.** *If μ is an S-node of **Type C**, then G_μ admits a pipe and a rectangular drawing.*

Proof. Recall that $\ell(\mu) = 2$, $s_1 t_1 \in E(G_{\mu_1})$, $s_2 t_2 \in E(G_{\mu_2})$, and none of μ_1 or μ_2 is bad.

By Lemma 3, we can construct a drawing Γ_{μ_1} of G_{μ_1} and a drawing Γ_{μ_2} of G_{μ_2} such that Γ_{μ_1} is an $H1^\circ$ drawing and Γ_{μ_2} is a $D1^\circ$ drawing.

We show how to compose Γ_{μ_1} and Γ_{μ_2} into a pipe drawing Γ_P of G_μ ; refer to Fig. 5(e). The first three steps of the construction are exactly as in the proof of Lemma 5. To obtain Γ_P , we perform an \hat{s} -scaling and a \hat{t} -scaling of the obtained drawing of G_μ so that the bottom side of $S(s)$ and the bottom side of $S(t)$ lie below the bottom side of $S(s_1) = S(t_2)$.

Finally, we show how to compose Γ_{μ_1} and Γ_{μ_2} into a rectangular drawing Γ_R of G_μ ; refer to Fig. 5(b). In this case, we obtain Γ_R simply by scaling and translating drawing Γ_{μ_1} and Γ_{μ_2} so that $S(t_2) = S(s_1)$.

It is not hard to see that, by construction and by the choice of the canonical drawings of G_{μ_1} and G_{μ_2} , drawings Γ_P and Γ_R are a pipe drawing and a rectangular drawing of G_μ , respectively. This concludes the proof. ◀

B.2 Omitted Proofs of Section 4

In a path-tree, the *interior* vertices are the vertices other than *root*, ℓ , and r . In an almost-triconnected path-trees, every interior vertex has degree at least three.

► **Lemma 7.** *Any almost-triconnected path-tree admits an SPQ-decomposition.*

Proof. We induct on the height of the path-tree G .

If the tree in G has height 1, then the root is the only tree node. If there are only two path vertices, then G is simply a Q-node. Otherwise, it is a P-node. Let the path in G be p_1, p_2, \dots, p_k . Then G can be produced by merging $k - 1$ Q-nodes. The child T_i of the P-node will be the Q-node consisting of root r , left path vertex p_i , and right path vertex p_{i+1} .

If the tree in G has height greater than 1, then first suppose that the only path vertices *root* can see are ℓ and r . Then *root* must have exactly one child in T , since otherwise there would be at least one visible path vertex between each pair of adjacent children. So G is an S-node whose single child contains $G - \text{root}$. We then continue the decomposition recursively.

Otherwise *root* can see a path vertex $p \neq \ell, r$. Either there is an edge from *root* to p , or there is space to draw such an edge. The vertices *root* and p divide G into two components. Let p_{i_1}, \dots, p_{i_k} be the left to right sequence of path vertices visible from *root*. For each j , the vertices *root*, p_{i_j} , and $p_{i_{j+1}}$ define a subgraph G_j containing the path vertices inclusively in between p_{i_j} and $p_{i_{j+1}}$ and the tree vertices on paths in the tree from *root* to those path vertices. So G is a P-node with children consisting of G_j for $j = 1, \dots, k - 1$. Each of these children has a smaller height, so we continue the decomposition recursively. ◀

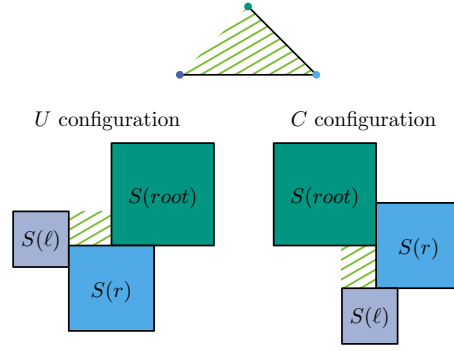
► **Lemma 8.** *Any almost-triconnected path-tree G without separating triangles and whose outer face is not a triangle admits a square-contact representation.*

Proof. As we construct the path-tree using the SPQ-decomposition, we maintain a square-contact representation for each node. For a path-tree H with root vertex *root*, leftmost path vertex ℓ , and rightmost path vertex r , the square-contact representation for H that we construct obeys the following invariant.

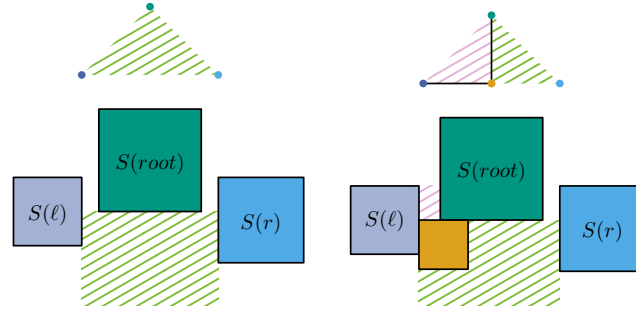
Inductive Invariant. There are two main cases we consider: either H has two path vertices or H has more than two path vertices. First if H has only two path vertices, then *root* may be connected to ℓ or r , but not both. Here we describe the invariant for when *root* is connected to r . The version where *root* is adjacent to ℓ is symmetric swapping ℓ with r and left with right throughout. If neither edge is present in H , then we can use either version of the invariant.

1. $S(\ell)$ appears to the left of $S(\text{root})$ and $S(r)$ appears directly to the right of $S(\ell)$ and is below $S(\text{root})$. The bottom of $S(\text{root})$ contacts the top of $S(r)$.
2. The top of $S(\ell)$ is vertically between the bottom of $S(\text{root})$ and one-third the distance to the top of $S(\text{root})$. The bottom of $S(\text{root})$ is vertically above the bottom border of $S(\ell)$.
3. If *root* and r are adjacent, then all other squares are inside the bounding box defined by extending the lines of the top of $S(\ell)$, the top of $S(r)$, the left of $S(\text{root})$ and the right of $S(\ell)$. We call this the $S(\text{root}), S(\ell)$ -bounding box.

Figure 9 illustrates the two-path-vertex, *root* adjacent to r , case of the invariant. Note that the square-contact representation can be rotated 90° such that $S(\ell)$ is below $S(\text{root})$ and $S(r)$ appears to the right of $S(\text{root})$ at the top of the square-contact representation. We call the original representation the U orientation and the rotated variant the C orientation for



■ **Figure 9** The invariant for a cycle-tree with two path vertices.



■ **Figure 10** The invariant for a cycle-tree with more than two path vertices.

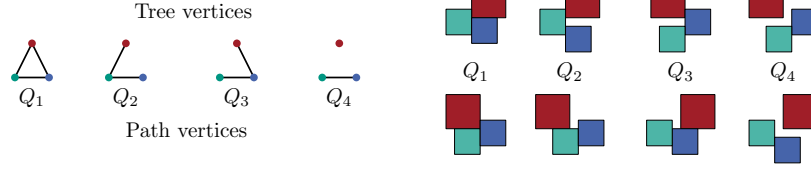
the shape formed by $S(\ell)$, $S(\text{root})$, and $S(r)$. The interior squares are fit into the “concavity” of the letter for the orientation.

If H has more than two path vertices, then:

1. $S(\ell)$ and $S(r)$ have their top on the same horizontal line.
2. $S(\ell)$, $S(\text{root})$, and $S(r)$ appear in that order from left to right with the tops of $S(\ell)$ and $S(r)$ between the bottom of $S(\text{root})$ and one-third the distance to the top of $S(\text{root})$ and the bottoms of $S(\ell)$ and $S(r)$ are below the bottom of $S(\text{root})$.
3. If ℓ and root are adjacent, then the right border of $S(\ell)$ touches the left border of $S(\text{root})$. If ℓ and root are not connected, then there is a horizontal gap between the right border of $S(\ell)$ and the left border of $S(\text{root})$. This is symmetric for the r and root connection.
4. If H is a P-node and the leftmost (or rightmost) child being merged has only two path vertices, then other squares are allowed inside the $S(\text{root})$, $S(\ell)$ -bounding box.
5. All other squares are drawn in the region below $S(\text{root})$, to the right $S(\ell)$, and to the left of $S(r)$.
6. Only interior squares contacting $S(\text{root})$ may touch the horizontal line extending out from the bottom of $S(\text{root})$. Only squares contacting $S(\ell)$ may touch the line extending out from the right of $S(\ell)$. Only squares contacting $S(r)$ may touch the line extending out from the left of $S(r)$.

Figure 10 illustrates the three-path-vertex case of the invariant. Together the two cases of this invariant guarantees the drawings for S-nodes and P-nodes resembles Fig. 7.

We now show how to construct a square-contact representation Γ for a path-tree G by inductively constructing a square-contact representation Γ_x that obeys the invariant for each node x in the decomposition. Let root_x be the root vertex of the tree vertices, ℓ_x be the



■ **Figure 11** The four possible path-trees for a Q-node and their square-contact representations.

leftmost path vertex, and r_x be the rightmost path vertex for a decomposition node x . We may drop subscripts when the decomposition node is clear.

First, [Figure 11](#) shows square-contact representations for each Q-node type obeying the invariant for graphs with two path vertices.

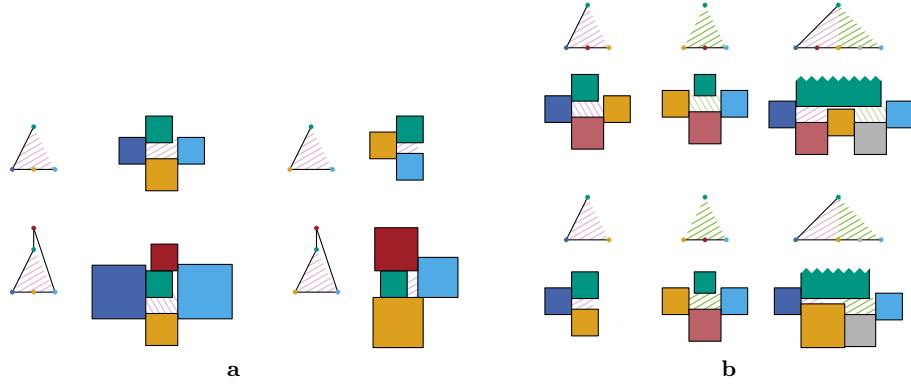
Handling S-nodes If x is an S-node that has just 2 path vertices with child node c , then $root_x$ cannot have edges to both ℓ_x and r_x , otherwise the three vertices form a separating triangle. If $root_x$ is adjacent to ℓ choose the orientation of Γ_c that places $S_{\Gamma_c}(r)$ below $S_{\Gamma_c}(root_c)$. Then construct Γ_x by drawing a square for x of the same size as $S_{\Gamma_c}(root_c)$ directly on top of $S(root_c)$ and perform $\hat{\ell}$ -scaling until its top is vertically between the bottom of $S(root_x)$ and one-third of the way to the top of $S(root_x)$. Γ_c may not have had an adjacency between $root_c$ and ℓ , in which case we \hat{root}_x -scale until its left contacts the right of $S(\ell)$. The case when $root_x$ is adjacent to r can be handled symmetrically. Finally when $root_x$ is adjacent to neither ℓ nor r , we can construct a case where there is a $root_x, \ell$ edge and then perform a slight negative \hat{root}_x -scaling to remove the extra contact.

If x is an S-node with at least 3 path vertices and child node c , then constructing the square-contact representation is much simpler. Γ_c obeys the second case of the invariant. Therefore in Γ_c , $S_{\Gamma_c}(\ell)$ appears on the left of the drawing and $S_{\Gamma_c}(r)$ appears on the right of the drawing with the other squares appearing between them. To construct Γ_x , start with Γ_c and place a new square for $root_x$ on the top of $S(root_c)$ of equal size. If $root_x$ is adjacent to ℓ , \hat{root}_x -scale until the left border is vertically in line with the right border of $S(\ell)$. If $root_x$ is adjacent to r , \hat{root}_x -scale until the right border is vertically in line with the left border of $S(r)$. Finally $\hat{\ell}$ -scale and \hat{r} -scale until their top borders lie between the bottom border of $S(root_x)$ and one-third of the way to the top of $S(root_x)$. It is possible $root_c$ was adjacent to ℓ or r and $root_x$ is not, if so we perform a slight negative \hat{root}_x or \hat{root}_x -scaling to remove the contact.

Every contact in Γ_c is preserved in Γ_x , because every square in Γ_c lies below the one-third line of $S_{\Gamma_c}(root_c)$. The only new contacts required in Γ_x are those involving $root_x$ which must contact $root_c$ and may contact ℓ or r . The placement of $S_{\Gamma_x}(root_x)$ guarantees contact with $S_{\Gamma_x}(root_c)$ and the scaling of $S_{\Gamma_x}(root_x)$ introduces contacts with $S_{\Gamma_x}(\ell)$ and $S_{\Gamma_x}(r)$ if needed. By construction Γ_x obeys the invariant.

Handling P-nodes We handle a P-node x by repeatedly merging the square-contact representations for two adjacent children c_1 and c_2 . For the pair of graphs being merged, call the shared root vertex $root$, the leftmost path vertex ℓ , the path vertex they share in common m , and the rightmost path vertex r . We use the C configuration for every child node with just two path vertices, unless it is the leftmost child and has an edge to the right of the two path vertices or it is the rightmost child and has an edge to the left of the two path vertices.

The order we merge children requires some care. For any child in a C configuration,



■ **Figure 12** Examples of the square-contact construction of an S-node (a) and of a P-node (b).

prioritize merging it in the direction of its “concavity”, that is if $root$ is adjacent to ℓ then merge the child with its right sibling. We perform all of these prioritized merges before any others.

After recursively constructing Γ_{c_1} and Γ_{c_2} , scale the two representations such that $S_{\Gamma_{c_1}}(m)$ is the same size as $S_{\Gamma_{c_2}}(m)$.

If neither or both of Γ_{c_1} and Γ_{c_2} are C configurations, we perform additional scaling to guarantee the bottom of $S_{\Gamma_{c_1}}(root)$ and $S_{\Gamma_{c_2}}(root)$ are at the same height. To do so, take the side with the higher square bottom for $root$ and perform \vec{m} -scaling and then rescale down the drawing to keep $S_{\Gamma_{c_1}}(m)$ the same size as $S_{\Gamma_{c_2}}(m)$. Now replace the squares for $root$ with a new square sharing bottom left corners with $S_{\Gamma_{c_1}}(root)$ and bottom right corners with $S_{\Gamma_{c_2}}(root)$. In some cases, this new square overlaps the top interior of $S(m)$. So if it is needed, we translate $S(m)$ downwards either until its top is in line with the bottom of $S(root)$, if m and $root$ are adjacent, or until it is slightly below $S(m)$, if m and $root$ are not adjacent. The resulting square-contact representation has at least three path vertices and obeys the second case of the invariant.

Because of our merge ordering, if there is only one C configuration then $root$ must not be adjacent to m . If we attempted to perform the above procedure with such a C configuration, then the result would not obey our invariant because the square of an outer path vertices would be below $S(root)$.

When only one of Γ_{c_1} and Γ_{c_2} is a C configuration and $root$ is not adjacent to m , after overlaying $S_{\Gamma_{c_1}}(m)$ and $S_{\Gamma_{c_2}}(m)$ it is not easy to replace the $root$ squares with one larger square. Without loss of generality we assume Γ_{c_1} is the C configuration. In this case, we observe that because $root$ and m are not adjacent, $S_{\Gamma_{c_2}}(m)$ can be translated downwards to slightly below $S_{\Gamma_{c_2}}(root)$ without disturbing any square contacts. After performing this translation, we can \vec{m} -scale followed by rescaling down Γ_{c_1} to keep $S_{\Gamma_{c_1}}(m)$ and $S_{\Gamma_{c_2}}(m)$ the same size such that the bounding box containing the squares of interior vertices has height equal to the slight vertical distance between $S(m)$ and $S(root)$ in the other drawing. Now we can finish the construction by creating a new large square for $root$ in the same manner as the previous case.

The line $S(m)$ is scaled along in the P node construction is guaranteed by the invariant to only intersect squares that are already in contact with $S(m)$. Similarly the bottom of the new $S(root)$ sits along the line touched only by the tops of squares of interior vertices adjacent to $root$. The translation of $S(m)$ is also designed such that any square previously in

contact with it, will still be in contact after the translation. Therefore Γ_x is a square-contact representation for x . By construction Γ_x follows the invariant.

Figure 12 shows our construction for two S-nodes on the left and two P-nodes each with two children on the right. ◀

► **Theorem 3.** *Any 3-connected cycle-tree G without separating triangles and whose outer face is not a triangle admits a square-contact representation.*

Proof. Given a 3-connected cycle-tree graph G without separating triangles, we split it into two path-trees using the following method:

1. Root the tree in G arbitrarily.
2. Let v be a leaf vertex of the tree in G .
3. If v can see at least three path vertices, select v and a subsequence of three path vertices visible from v .
4. Otherwise travel upwards in the tree until reaching a vertex u that can see at least three path vertices
5. There are at most two path vertices connected to descendants of u in the tree. Select u and a subsequence of three path vertices visible from u that include the path vertices connected to the descendants of u .
6. Now in either case, we have selected one tree vertex r and three consecutive path vertices which in counter-clockwise order are p_1 , p_2 , and p_3 visible from r . Removing r , p_1 , and p_3 disconnects the cycle-tree into two subgraphs H_1 and H_2 where H_1 is the subgraph containing p_2 .
7. $G - H_1$ and $G - H_2$ are two path-trees that coincide on r , p_1 , and p_3 .

Figure 9 depicts using this method to obtain two path-trees from a cycle-tree. Because the outer face of G has at least four path vertices, $G - H_2$ has exactly three path vertices, and the two subgraphs share two path vertices, $G - H_1$ has at least three path vertices. The two graphs $G - H_1$ and $G - H_2$ are almost-triconnected path-trees and so by Lemma 7, both graphs can be constructed by our decomposition. Then using r as the root of both path-trees, Lemma 8 guarantees $G - H_1$ and $G - H_2$ have square-contact representations Γ_1 and Γ_2 respectively satisfying the second case of the invariant.

In particular, Γ_1 has $S_{\Gamma_1}(r)$ in between $S_{\Gamma_1}(p_3)$ on the left and $S_{\Gamma_1}(p_1)$ on the right while Γ_2 has $S_{\Gamma_2}(r)$ in between $S_{\Gamma_2}(p_1)$ on the left and $S_{\Gamma_2}(p_3)$ on the right. Our goal is to align the squares for r , p_1 , and p_3 in both drawings while not introducing in new square-contacts.

We construct such a square-contact representation $\Gamma = \Gamma(G)$ as follows:

1. Let $d_i(x, y)$ be the horizontal distance between $S_i(x)$ and $S_i(y)$.
2. Scale the entire drawings of Γ_1 and Γ_2 so that $d_1(p_1, p_3) = d_2(p_1, p_3)$.
3. Rotate Γ_2 by 180° and vertically align the right sides of the squares $S_{\Gamma_1}(p_1)$ and $S_{\Gamma_2}(p_1)$. Note that the left sides of the squares $S_{\Gamma_1}(p_3)$ and $S_{\Gamma_2}(p_3)$ are also vertically aligned.
4. If $d_1(r, p_1) = d_2(r, p_1)$ and $d_1(r, p_3) = d_2(r, p_3)$, then $S_{\Gamma_1}(r)$ and $S_{\Gamma_2}(r)$ are the same size and we translate Γ_2 vertically such that $S_{\Gamma_1}(r)$ and $S_{\Gamma_2}(r)$ overlap exactly.
5. If $d_1(r, p_1) \neq d_2(r, p_1)$ and without loss of generality $d_1(r, p_1) < d_2(r, p_1)$, then perform \hat{r} -scaling in Γ_2 until the distances are equal. If there were squares in the $S_{\Gamma_2}(r), S_{\Gamma_2}(p_1)$ -bounding box, then perform \hat{a} -scaling on the squares in the bounding box where a is the bottom right corner of the bounding box until the horizontal width of the bounding box is $d_1(r, p_1)$.
6. If $d_1(r, p_3) \neq d_2(r, p_3)$, perform the analogous scaling to make them equal too.

7. Perform \hat{p}_1 -scaling so that its top border is above the top of $S_{\Gamma_2}(p_1)$. Do the analogous scaling for $S_{\Gamma_1}(p_3)$.
8. Remove $S_{\Gamma_2}(r)$, $S_{\Gamma_2}(p_1)$, and $S_{\Gamma_2}(p_3)$.

After the final removal step, Γ has one square for each vertex in G . We prove for each edge uv in $G - H_1$ that $S_\Gamma(u)$ contacts $S_\Gamma(v)$ using some case analysis, but first observe that rotations and scalings of entire square-contact representations preserve square contacts so we only need consider cases where u or v was scaled. The only squares undergo scaling in Γ_1 or Γ_2 are the squares for r , p_1 , p_3 , and any vertices in the $S_i(r)$, $S_i(p_j)$ -bounding boxes.

- Without loss of generality if u is p_1 (or p_3) then $S_{\Gamma_1}(v)$ touches the right side of $S_{\Gamma_1}(p_1)$. When $S(p_1)$ is scaled, the resulting right border is an extension of the original. The left border of $S(v)$ contains $S_{\Gamma_1}(v)$, because any scaling $S_{\Gamma_1}(v)$ underwent (possibly because $v = r$ or v is in the $S_{\Gamma_1}(r)$, $S_{\Gamma_1}(p_1)$ -bounding box) holds at least one point in contact with $S_{\Gamma_1}(p_1)$.
- If u is r and v is not p_1 or p_3 , then v may be below r or in the $S_{\Gamma_1}(r)$, $S_{\Gamma_1}(p_1)$ -bounding box. If v is below r , then the contact is also preserved, because whenever $S(r)$ is scaled the bottom is a superset of the previous bottom.

This argument is nearly symmetric for an edge in $G - H_2$. The only difference to observe is that the squares $S_{\Gamma_2}(p_1)$ or $S_{\Gamma_2}(p_3)$ are removed in favor of $S_{\Gamma_1}(p_1)$ and $S_{\Gamma_1}(p_3)$. Other squares only contact $S_{\Gamma_2}(p_1)$ on the right and $S_{\Gamma_2}(p_3)$ on the left. After scaling $S_{\Gamma_1}(p_1)$ ($S_{\Gamma_1}(p_3)$), the right (left) border $S_{\Gamma_1}(p_1)$ ($S_{\Gamma_1}(p_3)$) contains the right (left) border of $S_{\Gamma_2}(p_1)$ ($S_{\Gamma_2}(p_3)$). Therefore every edge in G has proper contact in Γ .

We also observe that no new contacts were introduced by these steps. Because for $i = 1, 2$ and $j = 1, 3$ the top border of the $S_i(t)$, $S_i(p_j)$ -bounding boxes are below the one-third line on $S_i(t)$, the overlaying of $S_{\Gamma_1}(t)$ with $S_{\Gamma_2}(t)$ does not introduce any new contacts (other than overlapping squares for the same vertex).

Thus Γ is a proper square-contact representation of G . ◀